(Received 20 August 2023, Accepted 21 November 2023, Scheduled 27 November 2023)

Series-Fed Loop Antenna Arrays with an Expanded Bandwidth of Circular Polarization

Kazuhide Hirose[1,*], Susumu Tsubouchi[1], and Hisamatsu Nakano[2]

[1] College of Engineering, Shibaura Institute of Technology, Tokyo 135-8548, Japan
[2] Science and Engineering, Hosei University, Tokyo 184-8584, Japan

ABSTRACT: Three array antennas are analyzed to expand a 3 dB axial ratio bandwidth using the method of moments. First, we design reference and present antennas comprising loop elements with a perturbation segment and quasi-two sources for circular polarization. It is found that the reference and present antennas have an axial ratio bandwidth of 9% and a 3 dB gain drop bandwidth of 31% (35% for the axial ratio bandwidth), respectively. Subsequently, the present antenna is modified using a sequential rotation technique. It is revealed that the modified antenna shows a gain drop bandwidth of 45% (60% for the axial ratio bandwidth). The simulated results are verified with experimental ones.

1. INTRODUCTION

A circularly polarized (CP) beam was formed using a series-fed array antenna above the ground plane [1–7]. The antenna was constructed using resonant elements such as patches [1–5] and loops [6, 7]. A non-resonant spiral element was recently used, expanding a 3 dB axial ratio bandwidth up to 30% [8].

This paper aims to further expand the axial ratio bandwidth of a series-fed array antenna above the ground plane. We adopt a square loop element with quasi-two sources [9] to construct an array antenna for the first time. The radiation characteristics are evaluated based on the current distribution determined by the method of moments [10].

A technical novelty of this paper is that by using resonant loop elements, we attain an axial ratio bandwidth (31%) comparable to that of a non-resonant spiral element array. One of the reasons for the bandwidth expansion is that the present loop with quasi-two sources has a unique CP radiation mechanism, where two loop corners are excited with the same amplitude and a phase difference of 90° using a branched feedline vertical to the ground plane [see Figure 1(a)]. In contrast, a conventional CP loop has a perturbation segment [see Figure 2(a)] or shape deformation [11].

This paper contributes to the fact that mutual coupling effects of loops [12] are applied to a series-fed array antenna to realize an axial ratio bandwidth comparable to that of a non-resonant element array. In [12], the mutual coupling effects between two loops with quasi-two sources expand the axial ratio bandwidth of an isolated loop with quasi-two sources by a factor of 3. These significant effects are the working mechanism of the present loop element array. Note that the coupling effects study has been restricted to the case of two loops, and no study has applied the effects to a series-fed array antenna.

* Corresponding authors: Kazuhide Hirose (khirose@shibaura-it.ac.jp).

This paper first presents the radiation characteristics of the present and reference antennas shown in Figures 1 and 2. After showing bandwidth expansion, we modify the present antenna using a sequential rotation technique [6] to further increase the bandwidth.

2. PRESENT AND REFERENCE ANTENNAS

Figures 1 and 2 show the present and reference antennas' configurations and coordinate systems. Each antenna is composed of N square loop elements of perimeter P. The loops are located at height H above the ground plane and separated with a distance d in the x-direction. The loop elements are connected to a straight feedline F-T horizontal to the ground plane, whose left end F is excited by a coaxial line via a vertical wire F-F', and the right end T is open-circuited. Note that we rotate the loops on the $+y$ side by 180° for the loops on the $-y$ side [8]. Additionally, note that the antenna is made of wires with a radius of ρ [6–9].

For the present antenna to radiate a CP wave, a loop of $\#n$ has a branched feedline α_n/β_n-B_n-γ_n vertical to the ground plane [9]. The branch point B_n is located at height h_B above the ground plane, and the bottom end γ_n is connected to the feedline F-T at height h_L, as shown in Figure 1(a). In contrast, the reference loop has a perturbation segment of length ℓ for CP radiation, and a loop corner is connected to the coplanar feedline F-T, as shown in Figure 2(b).

The antenna is analyzed using our developed program based on the method of moments [6–9]. The ground plane size is assumed to be infinite, and image theory is applied in the analysis. The present and reference loop parameters [(P, h_B) and (P, ℓ)] are selected for CP radiation, and the loop distance d is chosen to form the radiation beam normal to the antenna plane. The other configuration parameters are fixed at those in [6, 8]: (N, H, ρ) = (4, λ_0/4, λ_0/200), where λ_0 is the free-space wave-

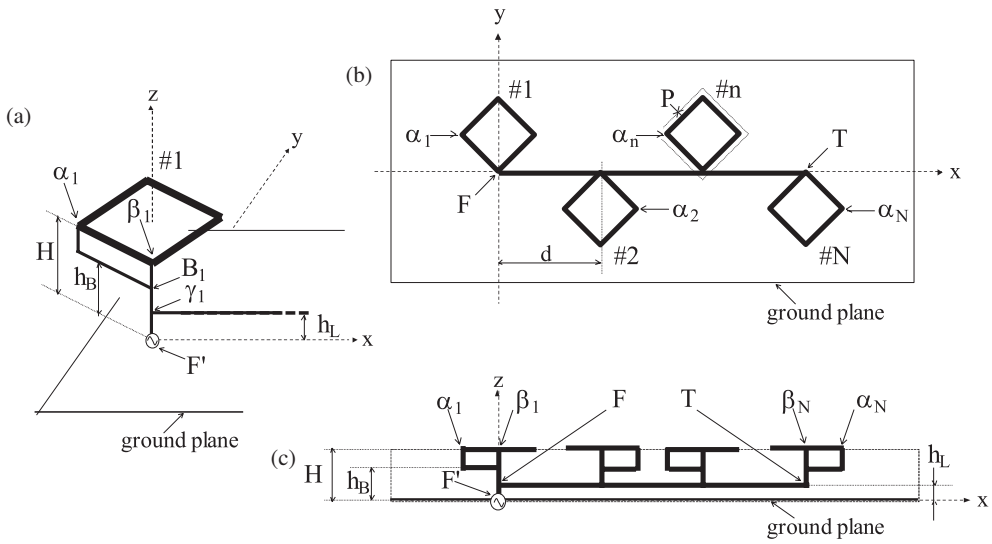

FIGURE 1. Present antenna with a straight feedline F-T horizontal to the ground plane. (a) Perspective view of a square loop element with a branched feedline $\alpha_1/\beta_1 - B_1 - \gamma_1$ vertical the ground plane. (b) Top view. (c) Side view.

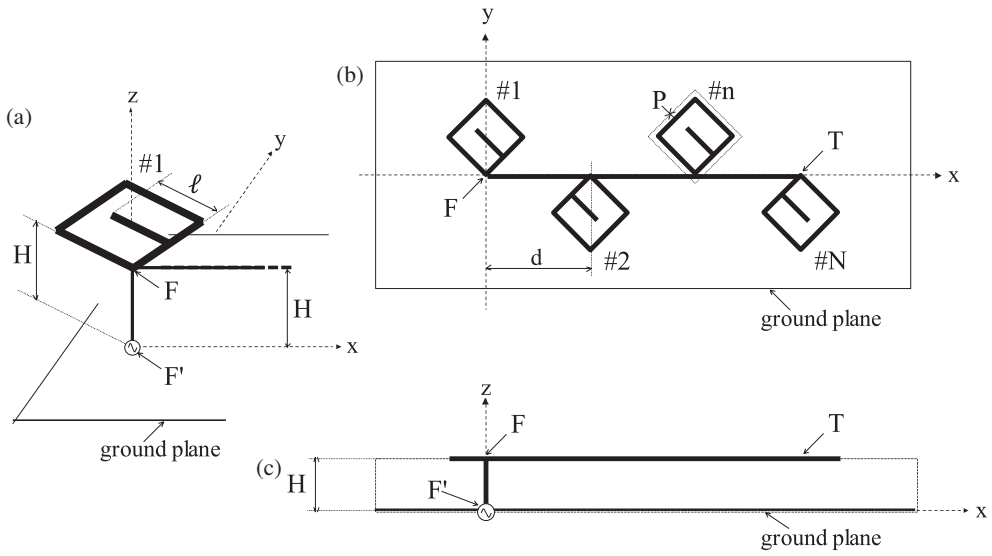

FIGURE 2. Reference antenna with a straight feedline F-T horizontal to the ground plane. (a) Perspective view of a square loop element with a perturbation segment of length ℓ. (b) Top view. (c) Side view.

length at a test frequency of f_0. Note that the horizontal feedline height of the present antenna is fixed to be $h_L = 0.02\lambda_0$ for input impedance matching the coaxial line.

Figure 3(a) shows the simulated radiation patterns of the present antenna with $(P, h_B, d) = (1.12\lambda_0, 0.09\lambda_0, 0.50\lambda_0)$. The radiation is decomposed into right- (E_R) and left-hand (E_L) CP wave components, which are shown with dotted and solid lines, respectively. It is observed that the antenna radiates a left-hand CP beam normal to the antenna plane. The half-power beam widths (HPBWs) are 23° and 55° in the $\phi = 0°$ and 90° planes, respectively. The gain is evaluated to be 12.6 dBi.

For comparison, Figure 3(b) shows the simulated radiation patterns of the reference antenna with $(P, \ell, d) = (1.20\lambda_0, 0.26\lambda_0, 0.54\lambda_0)$. It is seen that the CP beam is formed in the direction normal to the antenna plane. The HPBWs are 23° and 67° in the $\phi = 0°$ and 90° planes, respectively. The gain is 10.4 dBi.

The simulated frequency responses of the gain and axial ratio of the present and reference antennas are shown with solid and dotted lines in Figure 4. The present antenna is found to have a wider axial ratio bandwidth than the reference antenna. The axial ratio bandwidths of the present and reference antennas are 35% and 9%, respectively. Note that the present antenna has a 3 dB gain drop from the peak in the axial ratio bandwidth. When considering this, the overlap bandwidth is 31% $(0.85f_0 \sim 1.16f_0)$.

It is emphasized that the bandwidth (31%) of the present antenna is comparable to an array antenna composed of non-resonant spiral elements [8]. The bandwidth is comparable due

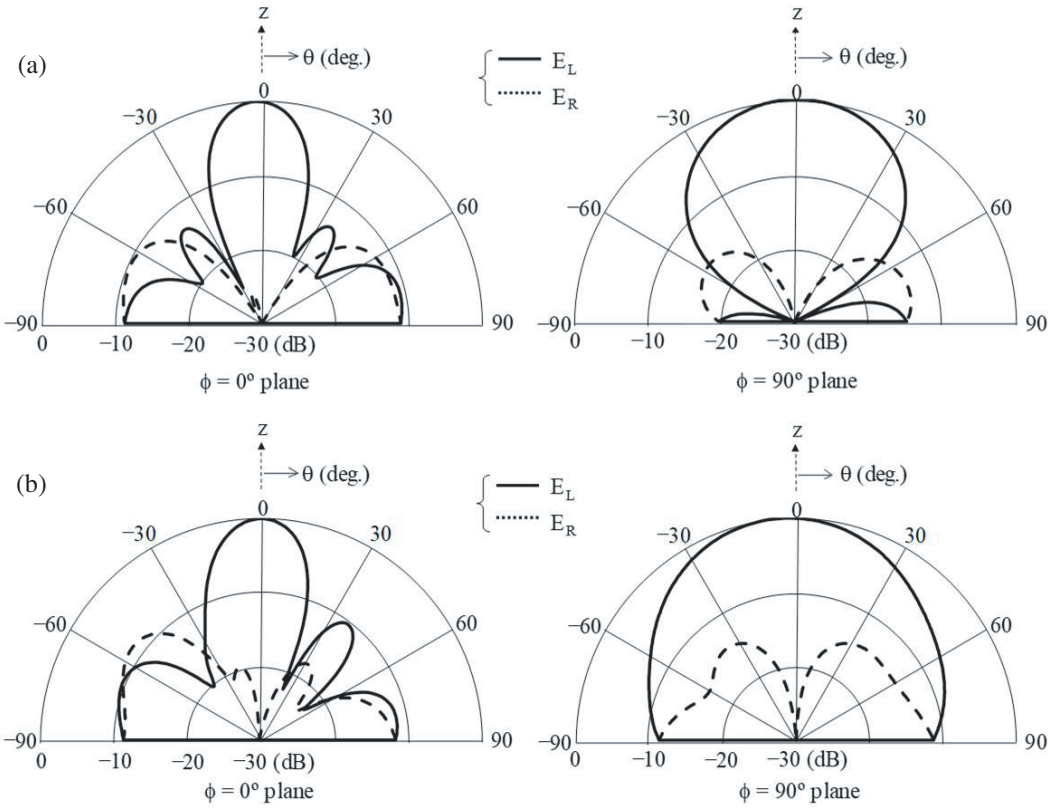

FIGURE 3. Simulated radiation patterns. (a) Present antenna. (b) Reference antenna.

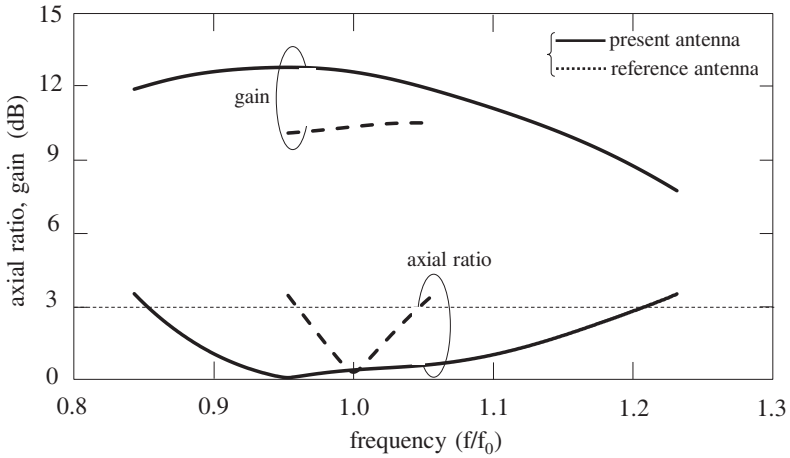

FIGURE 4. Simulated frequency responses of axial ratio and gain in the beam direction for the present and reference antennas.

to the mutual coupling effects of the loop elements since the axial ratio bandwidths of the isolated present and reference elements without an array environment are 12% [9] and 9% [6], respectively. In other words, the reference array antenna has the same axial ratio bandwidth as the isolated reference element. In contrast, the present array antenna's bandwidth is 2.6 times as wide as that of the isolated present element.

3. MODIFIED ANTENNA

So far, we have realized an axial ratio bandwidth comparable to that of a non-resonant element array. In this section, the bandwidth is further increased using a sequential rotation technique [6].

Figure 5 shows an antenna configuration modified with sequential rotation. The modification is performed in the following two stages:

1) The elements on the $-y$ side (Elements^{-y}) are shifted along the feedline F-T toward the feed point F by $\lambda_0/4$, as shown in Figure 6(a). This shift would make the excitation phase of Elements^{-y} lead by $90°(=\lambda_0/4\times 360°/\lambda_0)$. Note that we shorten the feedline F-T by $\lambda_0/4$, trimming an end part β_N-T.

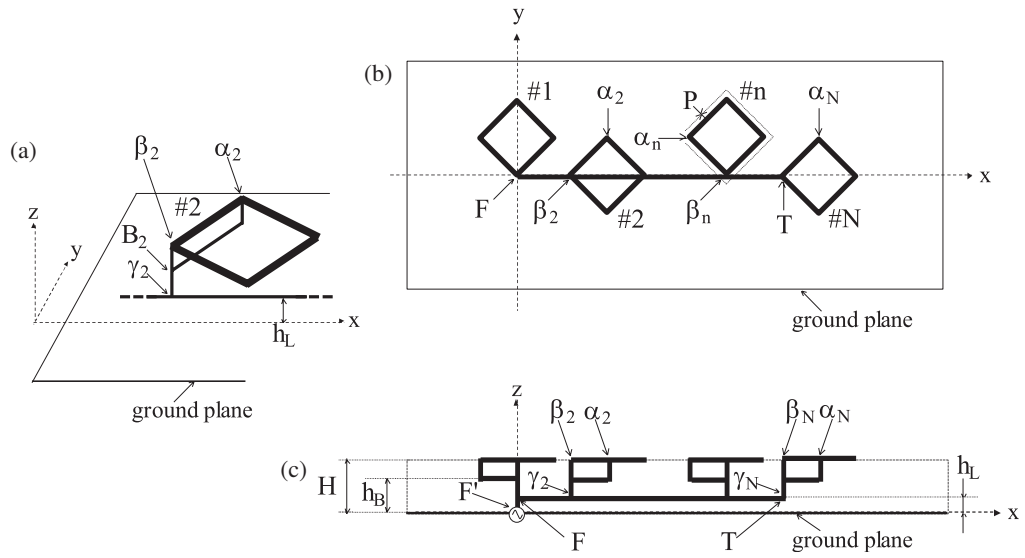

FIGURE 5. Modified antenna with a straight feedline F-T horizontal to the ground plane. (a) Perspective view of a square loop element with a branched feedline $\alpha_2/\beta_2 - B_2 - \gamma_2$ vertical to the ground plane. (b) Top view. (c) Side view.

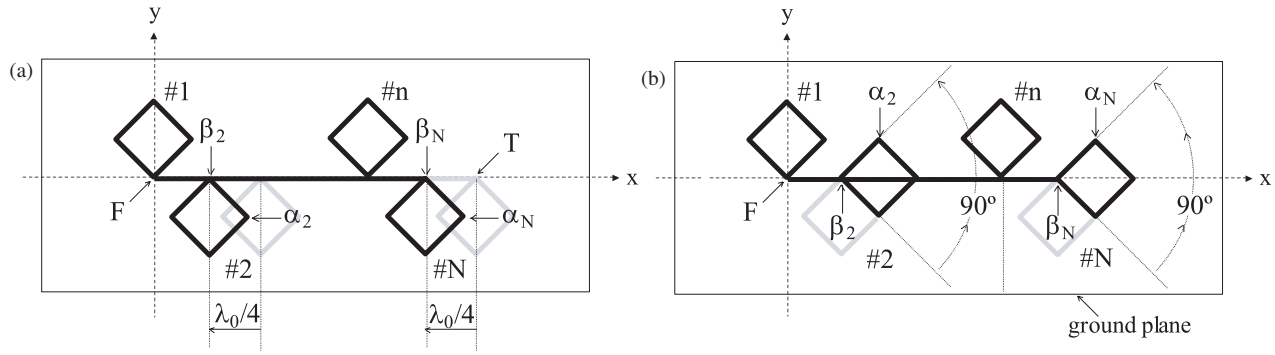

FIGURE 6. Modification process. (a) Element shift by $\lambda_0/4$ along a straight feedline F-T horizontal to the ground plane. (b) Element rotation by 90° for point β_n ($n = 2$ and N).

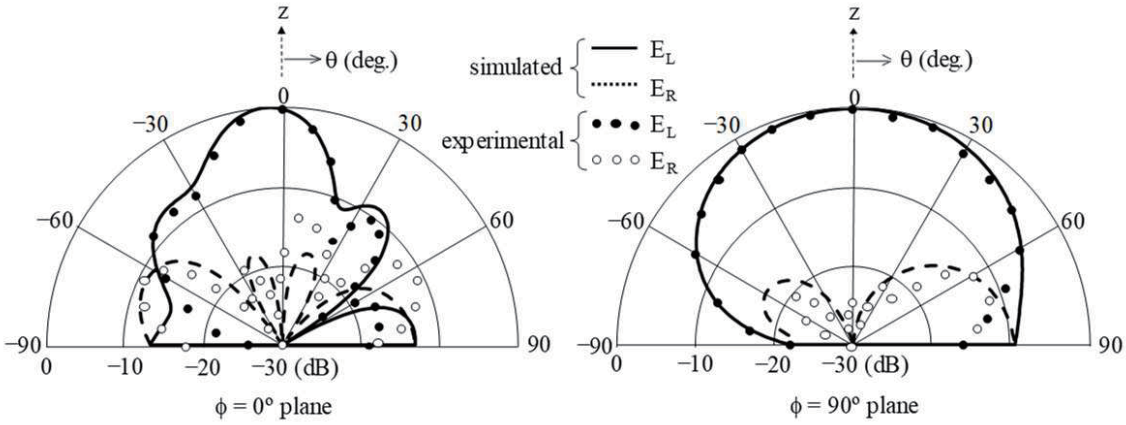

FIGURE 7. Radiation patterns of a modified antenna.

2) To compensate for the excitation phase lead, we rotate Elements^{-y} anticlockwise by 90°, as shown in Figure 6(b). This rotation causes the phase of partial radiation from Elements^{-y} to lag since the antenna radiates a left-hand CP wave, as shown in Figure 3(a) Note that this modification cannot be applied to the reference antenna in Section 2 since a rotated loop element of #2 would

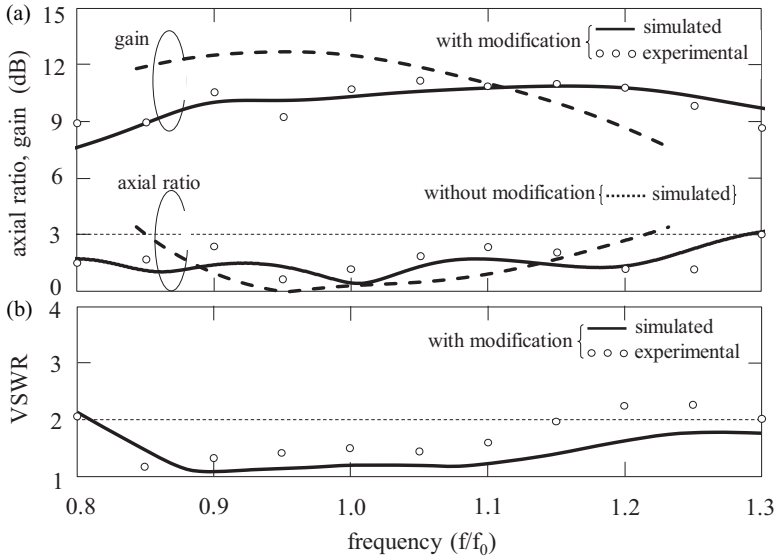

FIGURE 8. Frequency response of a modified antenna. (a) Axial ratio and gain in the beam direction. (b) VSWR.

TABLE 1. Comparisons with other studies.

Array element			Array type	3 dB axial ratio bandwidth (%)	Gain (dBi)	Operating frequency (GHz)	Matched termination
NR	Spiral	[8]	2×4	30	16.7	3	Not required
R	Patch	[1]	$1 \times 13 \times 4$	7.1	21.6	12.0	Required
			$1 \times 17 \times 4$	5.0	22.9	14.0	Required
		[2]	$1 \times 8 \times 15$	4	17.7	24	Required
		[3]	1×24	4	17.0	86	Required
		[4]	1×4	11.3	12.0	5	Required
			1×6	10.5	13.6	8	Required
		[5]	1×4	0.4	9.8	2	Not required
	Loop	[6]	2×4	18.9	15.8	3	Not required
		present	1×4	31	12.6	3	Not required
			1×4	45	10.2	3	Not required

(NR): non resonant; (R): resonant.

overlap the coplanar feedline F-T [see Figures 2(b) and (c)].

The modified antenna is designed for CP beam formation. For this, we select the loop parameters (P, h_B), holding the other configuration parameters at the values without modification in Section 2.

The solid and dotted lines in Figure 7 show the simulated radiation patterns for $(P, h_B) = (0.92\lambda_0, 0.08\lambda_0)$. It is observed that the CP beam is formed in the direction normal to the antenna plane. The HBPWs are 28° and 87° in the $\phi = 0°$ and 90° planes, respectively. The gain is 10.2 dBi.

The simulated gain and axial ratio versus frequency are shown with solid lines in Figure 8(a). For comparison, the results without modification in Section 2 are again shown with dotted lines. It is found that the modification leads to expansion of the axial ratio bandwidth, as expected. The modified antenna shows an axial ratio bandwidth of 60% (45% when considering the 3 dB gain drop: $0.81f_0 \sim 1.28f_0$). A solid line in Figure 8(b) shows the simulated frequency response of the VSWR concerning a 75 Ω coaxial line. The VSWR is less than 2 in the overlap bandwidth.

We perform experiments to verify the simulated results. The prototype is fabricated at $f_0 = 3$ GHz using a ground plane of $5\lambda_0 \times 5\lambda_0$, photographs of which are shown in Figure 9. The experimental results are shown with small circles and dots in Figures 7 and 8. The experimental results agree with the simulated ones.

Finally, our results are compared with those of similar studies. The comparisons are summarized in Table 1. It should be emphasized that the modified antenna has the widest axial ratio bandwidth. The bandwidth is widest because the present antenna without modification shows an axial ratio bandwidth (31%) comparable to that of a non-resonant spiral antenna array [8], as mentioned in Section 2. The spiral antenna array cannot be modified with the sequential rotation since the spiral has

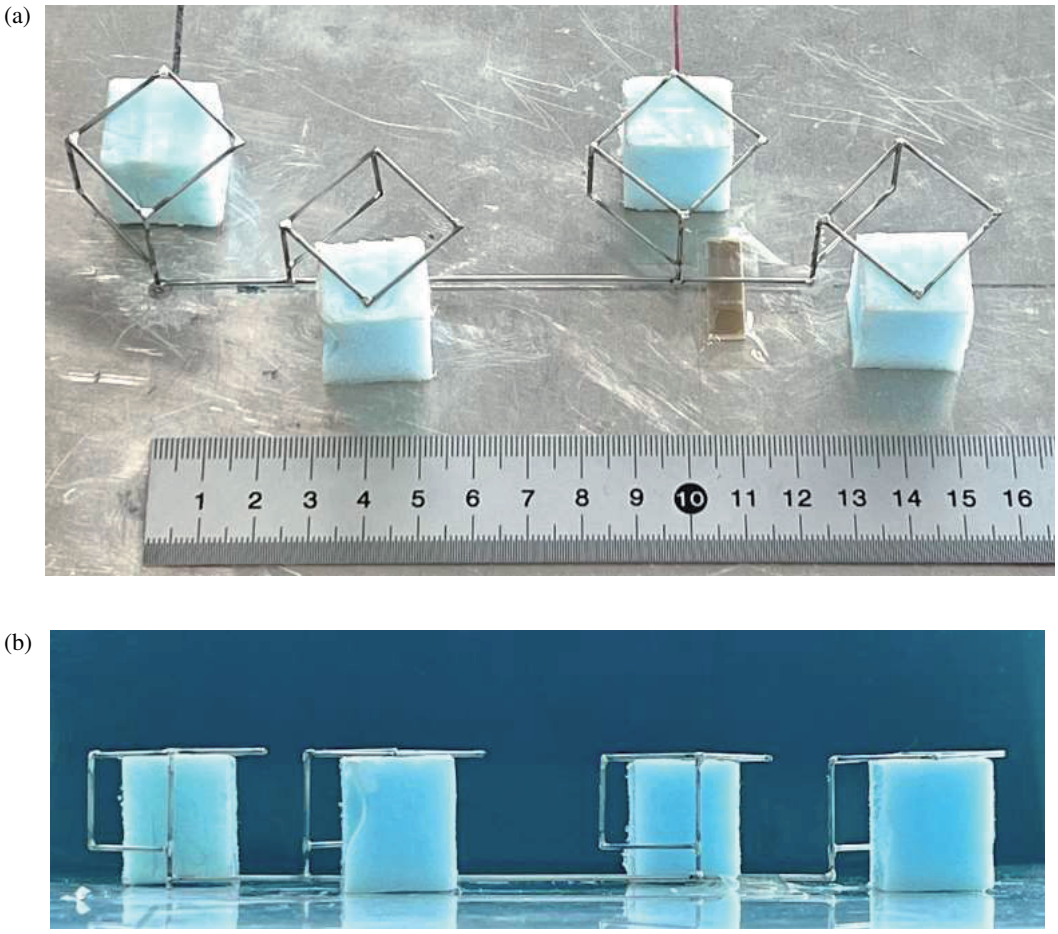

FIGURE 9. Prototype of a modified antenna. (a) Top view. (b) Side view.

TABLE 2. Antenna design methods with configuration parameters.

Configuration parameters classified			Reference antenna	Present antenna	Modified antenna
design methods	***part of antenna***	***parameters***			
optimization	loop	perimeter, $P(\lambda_0)$	1.20	1.12	0.92
		perturbation segment length, $\ell\ (\lambda_0)$	0.26	*not applied*	*not applied*
		branch point height, $h_B(\lambda_0)$	*not applied*	0.09	0.08
		distance between loops, $d(\lambda_0)$	0.54	0.50	0.50
	straight feedline F-T	height, $h_L\ (\lambda_0)$	*not applied*	0.02	0.02
automatic determination		length	$3d$	$3d$	$3d - \lambda_0/4$
precedent	the others	number of loops, N	4		
		loop height, $H(\lambda_0)$	1/4		
		wire radius, $\rho(\lambda_0)$	1/200		

a larger circumference ($1.3\lambda_0$) than the present loop ($0.9\lambda_0$), overlapping the adjacent spirals in the array.

Before concluding, we summarize our antenna design methods with configuration parameters. The summary is shown in Table 2, where the design methods are classified into three groups: optimization, automatic determination, and precedent.

The *optimization* is performed so that the loop element radiates a CP wave in a direction normal to the antenna plane. For this, the parameters (P, h_B) and (P, ℓ) of the present and reference loop elements are optimized for CP radiation [9 and 7], respectively, with the loop distance d being for the normal beam formation. We also optimize the height h_L of a straight feedline F-T for impedance matching [12]. Note that the reference antenna has a coplanar feedline F-T as a spiral element array [8], $h_L = H$.

The *automatic determination* means that the straight feedline length is automatically determined once the number of loops N and the distance d between the loops are determined. Note that

the feedline length of the modified antenna is shortened by $\lambda_0/4$ due to a loop shift of $\lambda_0/4$ along the feedline for the sequential rotation technique.

The *precedent* is set to facilitate the comparison with similar studies shown in Table 1. The reasons for the values of the number of loops N, loop height H, and wire radius ρ are as follows.

- $N = 4$: a unit element number of a sub-array used in an array antenna with an increased unit number, satisfying the gain and beam width required for an application.
- $H = \lambda_0/4$, at which an isolated loop element without an array environment shows wideband CP radiation.
- $\rho = \lambda_0/200$: satisfactory for an approximation in the moment method analysis, where antenna current is assumed to flow only in the wire axis direction.

4. CONCLUSION

We have designed reference and present loop antenna arrays to expand the 3 dB axial ratio bandwidth. It is found that the reference array has the same axial ratio bandwidth as an isolated loop element with a perturbation segment. In contrast, the present array's bandwidth is 2.6 times as wide as an isolated loop element with quasi-two sources. It is emphasized that a sequential rotation technique cannot be applied to the reference array since a rotated loop element would overlap with the coplanar feedline.

ACKNOWLEDGEMENT

The authors would like to thank Philip Sulter for his assistance in preparing this manuscript.

REFERENCES

[1] Nguyen-Trong, N., S. J. Chen, and C. Fumeaux, "High-gain dual-band dual-sense circularly polarized spiral series-fed patch antenna," *IEEE Open Journal of Antennas and Propagation*, Vol. 3, 343–352, 2022.

[2] Cao, Y., S. Yan, J. Li, and J. Chen, "A pillbox based dual circularly-polarized millimeter-wave multi-beam antenna for future vehicular radar applications," *IEEE Transactions on Vehicular Technology*, Vol. 71, No. 7, 7095–7103, Jul. 2022.

[3] Mishra, G., S. K. Sharma, and J.-C. S. Chieh, "A high gain series-fed circularly polarized traveling-wave antenna at w-band using a new butterfly radiating element," *IEEE Transactions on Antennas and Propagation*, Vol. 68, No. 12, 7947–7957, Dec. 2020.

[4] Bui, C. D., N. Nguyen-Trong, and T. K. Nguyen, "A planar dual-band and dual-sense circularly polarized microstrip patch leaky-wave antenna," *IEEE Antennas and Wireless Propagation Letters*, Vol. 19, No. 12, 2162–2166, Dec. 2020.

[5] Re, P. D. H., D. Comite, and S. K. Podilchak, "Single-layer series-fed planar array with controlled aperture distribution for circularly polarized radiation," *IEEE Transactions on Antennas and Propagation*, Vol. 68, No. 6, 4973–4978, Jun. 2020.

[6] Hirose, K., Y. Kikkawa, and H. Nakano, "Dual-loop arrays fed by coplanar parallel lines for wideband circular polarization," *IEEE Antennas and Wireless Propagation Letters*, Vol. 20, No. 4, 478–482, Apr. 2021.

[7] Hirose, K., M. Nakatsu, and H. Nakano, "A loop antenna with enlarged bandwidth of circular polarization — Its application in a comb-line antenna," *Progress In Electromagnetics Research C*, Vol. 105, 175–184, 2020.

[8] Hirose, K., Y. Tamura, M. Tsugane, and H. Nakano, "Coplanar series-fed spiral antenna arrays for enlarged axial ratio bandwidth," *Progress In Electromagnetics Research Letters*, Vol. 108, 1–8, 2023.

[9] Hirose, K., S. Tsubouchi, and H. Nakano, "A loop antenna with quasi-two sources for circular polarisation," *Electronics Letters*, Vol. 58, No. 6, 222–224, Mar. 2022.

[10] Harrington, R. F., *Field Computation by Moment Methods*, Macmillan, New York, NY, USA, 1968.

[11] Hirose, K., T. Yoshida, and H. Nakano, "Unbalanced-fed rectangular loop antennas for circular polarization," *IEEE Antennas and Propagation Society International Symposium*, 2018.

[12] Hirose, K., K. Nishino, and H. Nakano, "Dual-loop antennas with an expanded axial ratio bandwidth," *Electronics Letters*, Vol. 59, No. 8, 1–3, 2023. [Online]. Available: https://ietresearch.onlinelibrary.wiley.com/doi/abs/10.1049/ell2.12784